Send Orders for Reprints to reprints@benthamscience.net

Open Chemistry Journal, **2014**, *1*, 1-14

Variety of Crystal Structures of Chiral Schiff Base Lu(III)-Ni(II)/ Cu(II)/Zn(II) and the Related Complexes

Shingo Orita and Takashiro Akitsu*

Department of Chemistry, Faculty of Science, Tokyo University of Science, 1-3 Kagurazaka, Shinjuku-ku, Tokyo 162-8601, Japan

Abstract: New mononuclear $[Cu_2(L1)_2(H_2O)]2H_2O\cdot CH_3OH]$ (**cyCu**)$_2$, multinuclear $[Cu_2(L1)_2K_2][Ni(CN)_4]$ (**cyCuKNi**), and dinuclear $Ni(L1)Lu(NO_3)_3$ (**cyLuNi**), $Cu(L1)Lu(NO_3)_3$ (**cyLuCu**) and $Zn(L1)Lu[(NO_3)_2CH_3COO]CH_3OH$ (**cyLuZn**) complexes incorporating chiral Schiff base ligands were prepared and characterized by various techniques such as solid-state CD spectra, diffuse reflectance electronic spectra, IR spectra, and single crystal X-ray diffraction analysis. Crystal structures were also compared with previous ones, namely $[Cu(L2)](H_2O)$ (**diCu**), $Cu(L1)Gd(NO_3)_3$ (**cyGdCu**). Interestingly, determined crystal structures exhibited drastically different structural characteristics as regards coordination numbers, crystalline solvents, features and strain condition, nevertheless with little modification in 3d metal substitution and/or modified organic ligands. In this paper, comparison of common components of structures will be discussed systematically.

Keywords: 3d-4f complexes, chirality, crystal structures, Schiff base complexes, solid-state spectra.

INTRODUCTION

Chiral Schiff bases transition metal complexes, so-called salen-type ligands, are one of the most studied chiral catalysts in asymmetric synthesis because of their ability to act as chiral catalysts or as co-catalysts [1-7]. Moreover, their binuclear complexes containing transition metals and rare earth metals have gained importance from the viewpoint of special interest in photophysical and magnetic properties arising from interactions between metal ions as well as sole metal ions having suitable electronic states or unpaired electrons [8-19].

We have been interested in chiral salen-type 3d-4f binuclear complexes and have investigated structure-property correlation and their variety resulting from metal substitution and their combination [20-23]. In this work, in order to investigate structural features due to metal ions, we systematically investigate nine Schiff base complexes (abbreviated as **cyCu**, **cyCuKNi**, **cyLuNi**, **cyLuCu**, **cyLuZn**, **diLuNi** [20], **diLuCu** [20], and **diLuZn** [20]) and characterized them with diffuse reflectance electronic spectra, solid-state CD spectra, and X-ray crystal structure analysis. Additionally, these crystal structures were also compared with previously prepared two compounds, namely **diCu** [21] and **cyGdCu** [22]. Based on the basic structure of mononuclear **cyCu** having a common component, in which both four-coordinated and five-coordinated Cu(II) complexes are contained in a crystal, the variety and the reason of coordination geometries and structural features caused by systematic modifying ligands and substituting metal ions will be discussed (Fig. **1**).

*Address correspondence to this author at the Department of Chemistry, Faculty of Science, Tokyo University of Science, 1-3 Kagurazaka, Shinjuku-ku, Tokyo 162-8601, Japan; Tel: +81 3 5228 8271;
Fax: +81 3 5261 4361; E-mail: akitsu@rs.kagu.tus.ac.jp

EXPERIMENTAL SECTION

Materials

Chemicals of the highest commercial grade available (solvents are from Kanto Chemical, organic compounds are from Tokyo Chemical Industry and metal sources from Wako and Aldrich) were used as received without further purification.

Preparation of cyGdCu

Single crystals suitable for X-ray analysis of **cyGdCu** were prepared according to the procedure given in the literature [22].

Preparation of cyCu

To a solution of **cyGdCu** (0.0060 g, 0.0075 mmol) dissolved in methanol (1.5 mL), a solution of potassium tetracyano nickel(II) hydrate (0.0019 g, 0.0075 mmol) dissolved in water (1.5 mL) was added and stirred for 24 h at 298 K. The aqueous solution of potassium tetracyano nickel(II) hydrate played a role in promoting crystallization of good single crystals of **cyCu**. Purple needle crystals suitable for X-ray crystallography were obtained from the resulting solution (yield 0.0011 g, 32.03 %). Yield 0.0011 g (32.03 %). IR (KBr (cm^{-1}): 426 (w), 463 (w), 506 (w), 560 (m), 600 (m), 668 (w), 732 (s), 781 (w), 881 (w), 921 (w), 977 (m), 1025 (m), 1108 (w), 1163 (w), 1224 (s), 1242 (s), 1321 (s), 1354 (m), 1390 (w), 1442 (s), 1473 (s), 1542 (m), 1600 (s), 1626 (s) (C=N), 2928 (s), 3504 (s).

Preparation of cyCuKNi

Under N_2 atmosphere at 298 K, treatment of tetraethylammonium perchlorate (0.640 g, 2.00 mmol) and potassium tetracyano nickel(II) hydrate (0.259 g, 1.00 mmol) in methanol (50 mL) for 72 h gave rise to tetraethylammonium

1874-8422/14

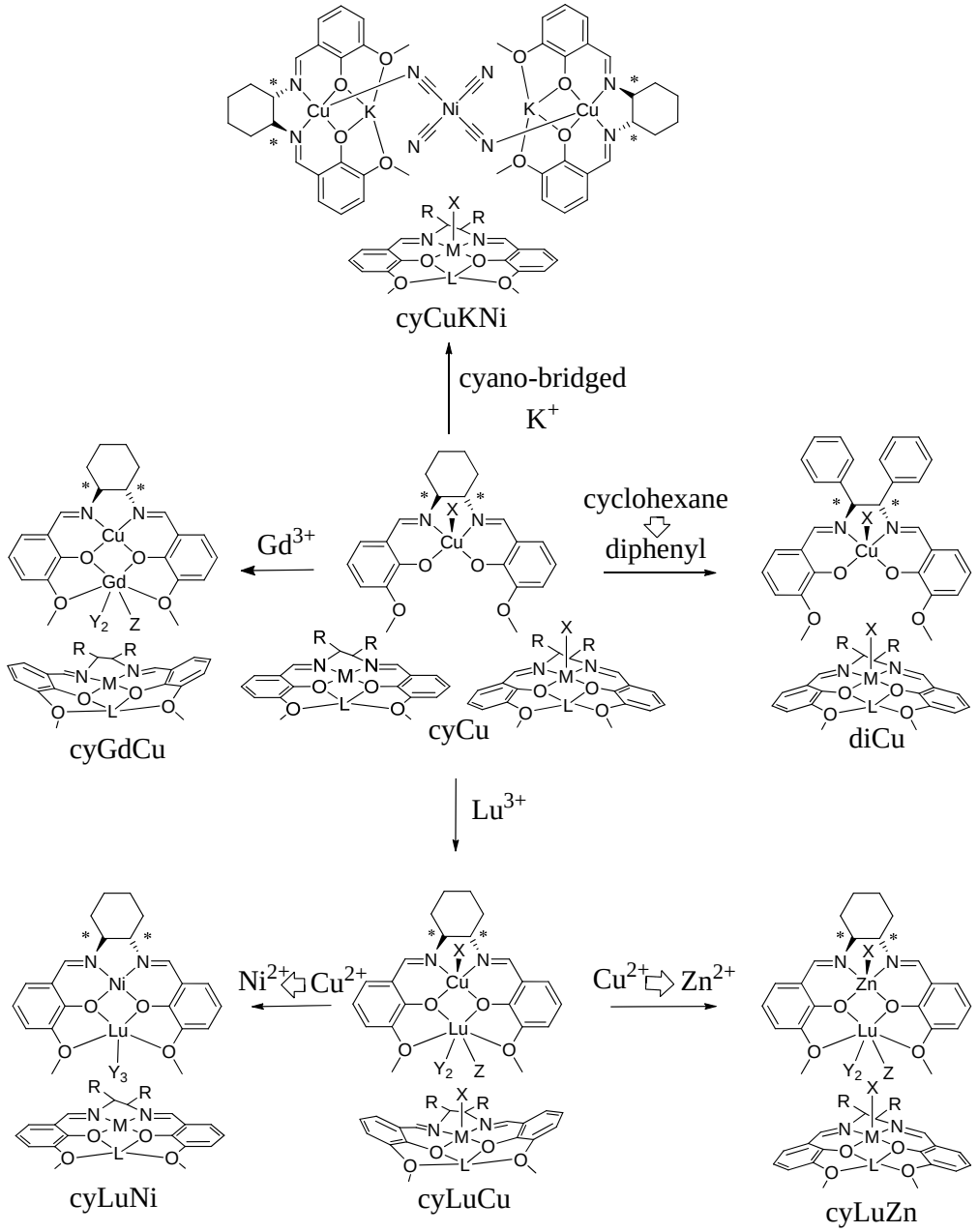

Fig. (1). Structures of complexes and summary of structural features determined.

tetracyanonickel(II) hydrate (a precursor). To a 5 mmol/L methanol solution of potassium tetracyanonickel(II) hydrate (1.5 mL), a precursor **cyGdCu** (0.0060 g, 0.0075 mmol) in methanol (1.5 mL) was added and stirred for 24 h at 298 K. A few grains of brown prismatic crystals suitable for X-ray crystallography were obtained from the resulting solution. Yield 0.0013 g (15.41 %). IR (KBr (cm^{-1}): 562 (s), 668 (w), 748 (s), 853 (w), 970 (m), 1027 (w), 1082 (m), 1212 (s), 1242 (s), 1318 (m), 1440 (s), 1473 (s), 1542 (m), 1629 (s) (C=N), 2118 (m) (C≡N), 2839 (w), 2933 (w), 3423 (s).

Preparation of cyLuNi

To a solution of *o*-vanillin (0.305 g, 2.00 mmol) dissolved in methanol (60 mL), (*1R,2R*)-(-)-1,2-cyclohexanediamine (0.114 g, 1.00 mmol) was added and stirred at 313 K for 2 h to give yellow solution of ligand(L1). Nickel(II)acetate tetrahydrate (0.2545 g, 1.00 mmol) was added to the resulting solution to yield muddy brown solution of the complex. After stirring at 313 K for 3 h, lutetium(III)nitrate hexahydrate (0.3642 g 1.00 mmol) was added to the resulting solution and the mixed solution was refluxed for 4 h at 373 K. After cooling the solution, the resulting orange compound was filtered and recrystallized from methanol/diethyl ether to obtain single crystals. Yield 0.5732 g (71.64 %). Anal. Found: C, 33.22 ; H, 2.91 ; N, 8.61 %. Calc. for $C_{22}H_{24}LuN_5NiO_{13}$: C, 33.02 ; H, 3.02 ; N, 8.75 %. IR (KBr (cm^{-1}):566 (w), 598 (w), 681 (w),740 (m), 786 (w), 810 (w), 869 (w), 964 (m), 1036 (m), 1077 (m), 1168 (w), 1232 (s), 1321 (s), 1383 (m), 1478 (s), 1520 (s), 1619 (s) (C=N), 1700 (s), 2328 (w), 2944 (w), 3401 (s).

Preparation of cyLuCu

To a solution of *o*-vanillin (0.305 g, 2.00 mmol) dissolved in methanol (60 mL), (*1R,2R*)-(-)-1,2-cyclohexanediamine (0.114 g, 1.00 mmol) was added and stirred at 313 K for 2 h to give yellow solution of ligand (L1). Copper(II)acetate hydrate (0.2027 g, 1.00 mmol) was added to the resulting solution to yield muddy purple solution of the complex. After stirring at 313 K for 3 h, lutetium(III)nitrate hexahydrate (0.3610 g, 1.00 mmol) was added to the resulting solution and the reaction was refluxed for 4 h at 373 K. The solution was evaporated under reduced pressure, and deep brown compound was yielded. This compound was filtered and recrystallized from methanol/diethyl ether to give crystals. Yield 0.5962 g (74.06 %). Anal. Found: C, 33.14; H, 3.06; N, 6.80 %. Calc. for $C_{22}H_{24}LuN_5CuO_{13}$: C, 32.83; H, 3.01; N, 8.70 %. IR (KBr (cm^{-1}): 533 (w), 650 (w), 740 (m), 855 (w), 949 (m), 1019 (m), 1070 (m), 1221 (s), 1303 (s), 1383 (m), 1468 (s), 1521 (m), 1630 (s) (C=N), 1652 (s), 2328 (w), 2943 (m), 3399 (s).

Preparation of cyLuZn

To a solution of *o*-vanillin (0.305 g, 2.00 mmol) dissolved in methanol (60 mL), (*1R,2R*)-(-)-1,2-cyclohexanediamine (0.114 g, 1.00 mmol) was added and stirred at 313 K for 2 h to give a ligand (L1). Zinc(II)acetate tetrahydrate (0.2243 g, 1.00 mmol) was added to the resulting solution to yield light-yellow solution of the complex. After stirring at 313 K for 3 h, lutetium(III) nitrate hexahydrate (0.3526 g, 1.00 mmol) was added to the resulting solution and the reaction was refluxed for 4 h at 373 K. The solution was evaporated under reduced pressure, and yellow compound was obtained. This compound was filtered and recrystallized from methanol/diethyl ether to obtain single crystals containing (nonstoichometric) CH_4O solvent suitable for X-ray analysis. Yield 0.5732 g (68.57 %). Anal. Found: C, 35.86; H, 3.60; N, 6.62 %. Calc. for $C_{25}H_{31}LuN_4ZnO_{13}$: C, 35.92; H, 3.74; N, 6.70 %. IR (KBr (cm^{-1}): 444 (w), 537 (w), 566 (w), 624 (w), 665 (m), 739 (s), 781 (w), 812 (w), 857 (m), 888 (w), 949 (s), 1015 (s), 1073 (m), 1165 (w), 1221 (s), 1268 (s), 1165 (m), 1380 (w), 1384 (m), 1476 (s), 1534 (s), 1556 (m), 1630 (m) (C=N), 1656 (m), 2942 (m), 2424 (s), 3403 (s).

Preparation of diCu

Single crystals suitable for X-ray analysis of **diCu** were prepared according to the procedure given in the literature [21].

Physical Measurements

Elemental analyses (C, H, N) were carried out with a Perkin-Elmer 2400II CHNS/O analyzer at Tokyo University of Science. Infrared spectra were recorded using KBr pellets on a JASCO FT-IR 4200 plus spectrophotometer in the range of 4000-400 cm^{-1} at 298 K. Diffuse reflectance spectra were measured on a JASCO V-570 UV/VIS/NIR spectrophotometer equipped with an integrating sphere in the range of 800-200 nm at 298 K. Circular dichroism (CD) spectra were measured as KBr pellets on a JASCO J-820 spectropolarimeter in a range of 800-300 nm at 298 K. Fluorescence spectra in the solid state were recorded on a JASCO FP-6200 spectrophotometer at 298 K.

X-Ray Crystallography

Prismatic single crystals of purple **cyCu**, brown **cyGdCu**, brown **cyCuKNi**, orange **cyLuNi**, purple **cyLuCu**, pale yellow **cyLuZn,** and green **diCu** were glued on top of a glass fiber and coated with a thin layer of epoxy resin. Intensity data were collected on a Bruker APEX2 CCD diffractometer with graphite monochromated Mo Kα radiation (λ = 0.71073 A). Data analysis was carried out with a SAINT program package. The structures were solved by direct methods with a SHELXS-97 [24] and expanded by Fourier techniques and refined by full-matrix least-squares methods based on F^2 using the program SHELXL-97 [24]. A multi-scan absorption correction was applied by a program SADABS. All non-hydrogen atoms were readily located and refined by anisotropic thermal parameters. All hydrogen atoms were located at geometrically calculated positions and refined using riding models.

The crystallographic data for "**cyCu**, **cyGdCu**, and **CyCuKNi**", "**cyLuM** (M=Ni, Cu, and Zn)", and "**diCu**"are summarized in Tables **1**, **2**, and **3**, respectively.

RESULTS AND DISCUSSION

Structure Description of cyCu

Complex **cyCu** crystallizes in monoclinic, space group $P2_1$ with Z = 2. As shown in Figs. (**2**) and S1, the asymmetric unit of **cyCu** contains crystallographically two independent molecules of four-coordinated and five coordinated mononuclear Cu(II) complexes. One of the Cu(II) complex affords a four-coordinated square planar [CuN_2O_2] geometry with the four donor atoms of the tetradentete Schiff base forming the equatorial plane with Cu1–N1, Cu1-N2, Cu1-O2, and Cu1-O4 distances ranging from 1.8946(19) to 1.937(2) Å (Table **4**).

The other Cu(II) complex affords a five-coordinated square pyramidal [CuN_2O_3] geometry with additional aqua ligand occupying the axial sites with Cu2–N3, Cu2-N4, Cu2-O6, and Cu2-O8 distances ranging from 1.9114(19) to 1.951(2) Å and axial O atom from coordinate aqua ligand with Cu2–O9 distance of 2.453(2) Å (Table **4**). The displacement of Cu1 and Cu2 from the A-plane and A'-plane (Fig. **3**) is 0.0198(13) Å and 0.1407(13) Å, respectively. The chiral (*1R,2R*)-(-)-1,2-cyclohexanediamine moieties adopt a λ configuration with torsion angles N1-C9-C20-N2 = -47.2(3)° and N3-C31-C42-N4 = -45.8(3)°, respectively.

The dihedral angles between the B-plane and C-plane and between the B'-plane and C'-plane are 13.86(6) and 5.45(5)°, respectively. The angles between the A-plane and B-plane and between the A'-plane and B'-plane are 9.65(4) and 8.77(4)°, respectively. And the angles between the A-plane and C-plane and between the A'-plane and C'-plane are 4.21(6) and 3.42(3)°, respectively. Moreover, the angles between the A-plane and D-plane, between the A-plane and E-plane, and between the D-plane and E-plane are 8.24(4), 6.82(6), and 14.65(6)°, and between the A'-plane and D'-plane, between the A'-plane and E'-planes, and between the D'-plane and E'-plane are 7.84, 4.81, and 6.53°, respectively.

Table 1. Crystal data and structure refinement for cyCu, CyGdCu, and cyCuKNi.

Complex	cyCu CCDC=978339	cyGdCu CCDC=978341	cyCuKNi CCDC=978340
Empirical formula	$C_{45}H_{58}N_4Cu_2O_{12}$	$C_{22}H_{24}GdN_5CuO_{13}$	$C_{48}H_{48}Cu_2NiK_2N_8O_8$
Formula weight	974.03	787.25	1128.93
Temperature (K)	173(2)	173(2)	173(2)
Crystal system	Monoclinic	Monoclinic	Triclinic
Space group	$P2_1$(#4)	$P2_1$(#4)	$P1$(#1)
a (Å)	12.5607(18)	11.2519(14)	10.3332(18)
b (Å)	13.996(2)	15.2843(19)	11.896(2)
c (Å)	13.590(2)	15.8759(19)	12.022(4)
α(°)			106.403(3)
β(°)	114.296(2)	105.2850(10)	107.050(3)
γ(°)			109.936(2)
V (Å^3)	2177.6(6)	2633.7(6)	1201.9(5)
Z	2	4	1
Crystal size (mm)	0.11x0.09x0.06	0.21x0.20x0.19	0.25x0.23x0.10
Density (calculated) (g/cm^{-3})	1.486	1.985	1.560
Absorption coefficient (mm^{-1})	1.045	3.382	1.500
F(000)	1020	1552	580
Θ range for data collection(°)	2.20 to 27.55	2.30 to 27.47	2.13 to 27.61
Limiting indices	-14<=h<=16, -17<=k<=17, -11<=l<=17	-14<=h<=6, -19<=k<=19, -20<=l<=20	-13<=h<=12, -15<=k<=14, -11<=l<=15
Reflections collected	12035	14537	6590
Independent reflections	8926 [R(int) = 0.0202]	10930 [R(int) = 0.0585]	5758 [R(int) = 0.0172]
Completeness to θ	99.6 %	99.5 %	97.2 %
Refinement method	Full-matrix least-squares on F^2	Full-matrix least-squares on F^2	Full-matrix least-squares on F^2
Data/restraints/parameters	8926 / 7 / 599	10930 / 1 / 762	5758 / 3 / 628
Goodness-of-fit on F^2	1.024	0.921	1.372
Final R indices [I>2sigma(I)]	R1 = 0.0335, wR2 = 0.0767	R1 = 0.0457, wR2 = 0.1136	R1 = 0.0399, wR2 = 0.0653
R indices (all data)	R1 = 0.0404, wR2 = 0.0794	R1 = 0.0461, wR2 = 0.1142	R1 = 0.0595, wR2 = 0.0687
Absolute structure parameter	0.023(9)	-0.050(11)	0.449(19)
Largest diff. peak and hole (e Å^{-3})	0.801 and -0.656	2.490 and -1.632	0.419 and -0.544

Table 2. Crystal data and structure refinement for cyLuM(M=Ni, Cu, Zn).

Complex	cyLuNi CCDC=978343	cyLuCu CCDC=978342	cyLuZn CCDC=978344
Empirical formula	$C_{22}H_{24}LuN_5NiO_{13}$	$C_{22}H_{24}LuN_5CuO_{13}$	$C_{25}H_{31}LuN_4ZnO_{13}$
Formula weight	800.14	804.97	835.88
Temperature (K)	173(2)	173(2)	173(2)
Crystal system	Triclinic	Monoclinic	Triclinic
Space group	*P*1(#1)	$P2_1$(#4)	*P*1(#1)
a (Å)	9.2894(7)	11.3230(10)	8.6140(5)
b (Å)	12.0897(9)	15.0586(13)	13.1481(7)
c (Å)	12.1846(9)	15.8854(14)	13.7513(8)
α(°)	101.6720(10)		85.4810(10)
β(°)	96.3530(10)	103.7560(10)	84.5190(10)
γ(°)	90.6220(10)		71.5330(10)
V (Å ^{3})	1331.10(17)	2630.9(4)	1468.90(14)
Z	2	4	2
Crystal size (mm)	0.18 0.11 0.06	0.16 0.12 0.09	0.16 0.12 0.11
Density (calculated) (g/cm^{-3})	1.996	2.032	1.890
Absorption coefficient (mm^{-1})	4.471	4.617	4.230
F(000)	788.0	1580.0	828
θrange for data collection(°)	2.17 to 27.51	2.29 to 27.62	2.27 to 25.03
Limiting indices	-12<=h<=11, -14<=k<=15, -15<=l<=7	-8<=h<=14, -19<=k<=14, -20<=l<=19	-9<=h<=10, -11<=k<=15, -14<=l<=16
Reflections collected	7330	14463	6845
Independent reflections	6365 [R(int) = 0.0446]	10366 [R(int) = 0.0179]	5825 [R(int) = 0.0553]
Completeness to θ	97.0 %	99.6 %	97.3 %
Refinement method	Full-matrix least-squares on F^2	Full-matrix least-squares on F^2	Full-matrix least-squares on F^2
Data/restraints/parameters	6365 / 45 / 761	10366 / 1 / 762	5825 / 483 / 803
Goodness-of-fit on F^2	0.852	1.009	1.030
Final R indices [I>2sigma(I)]	R1 = 0.0457, wR2 = 0.1132	R1 = 0.0230, wR2 = 0.0510	R1 = 0.0305, wR2 = 0.0799
R indices (all data)	R1 = 0.0474, wR2 = 0.1148	R1 = 0.0247, wR2 = 0.0514	R1 = 0.0316, wR2 = 0.0811
Absolute structure parameter	0.019(17)	0.024(7)	0.003(9)
Largest diff. peak and hole (e $Å^{-3}$)	3.248 and -2.170	0.794 and -0.906	2.073 and -1.147

The displacement of O9 from the F-plane is 0.6961(32) Å for the four-coordinated molecule taking planar structure (see Fig. **4**). Whereas the displacement of O10 from the F'-plane is 0.9007(33) Å for the five-coordinated molecule (see Fig. **4**). Since axial water ligands and crystalline water are in the same side, the overall molecule takes slightly distorted umbrella structure towards the opposite side of the axial ligand (see Fig. **5**).

Structure Description of cyGdCu

Complex **cyGdCu** crystallizes in monoclinic, space group $P2_1$ with Z = 4. As shown in Fig. (**6**) and S2, the

Gd(III) ion affords a ten-coordinated environment with distorted square pyramidal towards bridging nitrate ligands. While Cu(II) ion affords a four-coordinated square planar [CuN_2O_2] geometry with Cu1–N1, Cu1-N2, Cu1-O2, and Cu1-O4 distances ranging from 1.898(5) to 1.916(5) Å (Table **5**), the displacement of Cu1 from the A-plane is 0.0357(25) Å (see Fig. **3**). The chiral (*1R,2R*)-(-)-1,2-cyclohexanediamine moiety adopts a λ configuration, with torsion angle N1-C9-C20-N2 = -49.1(6)°.

Table 3. Crystal data and structure refinement for diCu.

Complex	diCu CCDC=978345
Empirical formula	$C_{30}H_{28}N_2CuO_5$
Formula weight	560.08
Temperature (K)	173(2)
Crystal system	Monoclinic
Space group	$P2_1$(#4)
a (Å)	12.3063(17)
b (Å)	9.5429(13)
c (Å)	22.516(3)
α(°)	
β(°)	98.227(2)
γ(°)	
V (Å ^{3})	2617.0(6)
Z	4
Crystal size (mm)	0.14 0.10 0.06
Density (calculated) (g/cm^{-3})	1.422
Absorption coefficient (mm^{-1})	0.878
F(000)	1164
θrange for data collection(°)	2.29 to 27.52
Limiting indices	-9<=h<=15, -12<=k<=11, -29<=l<=29
Reflections collected	14028
Independent reflections	9632 [R(int) = 0.0280]
Completeness to θ	99.0 %
Refinement method	Full-matrix least-squares on F2
Data/restraints/parameters	9632 / 1 / 705
Goodness-of-fit on F^2	0.930
Final R indices [I>2sigma(I)]	R1 = 0.0335, wR2 = 0.0799
R indices (all data)	R1 = 0.0494, wR2 = 0.0877
Absolute structure parameter	-0.024(10)
Largest diff. peak and hole (e Å^{-3})	0.396 and -0.446

Table 4. Selected bond lengths (Å) and angles(°) for cyCu.

Bond lengths			
Cu1-N1	1.930(2)	Cu2-N3	1.948(2)
Cu1-N2	1.937(2)	Cu2-N4	1.951(2)
Cu1-O2	1.8966(17)	Cu2-O6	1.9114(19)
Cu1-O4	1.8946(19)	Cu2-O8	1.9166(17)
		Cu2-O9	2.453(2)
Bond angles			
N1-Cu1-N2	85.08(10)	N3-Cu2-N4	84.37(9)
N1-Cu1-O2	94.53(9)	N3-Cu2-O6	93.02(9)
N1-Cu1-O4	167.89(11)	N3-Cu2-O8	175.17(11)
N2-Cu1-O2	170.41(11)	N4-Cu2-O6	167.30(11)
N2-Cu1-O4	93.68(9)	N4-Cu2-O8	92.83(8)
O2-Cu1-O4	88.68(7)	O6-Cu2-O8	88.86(8)

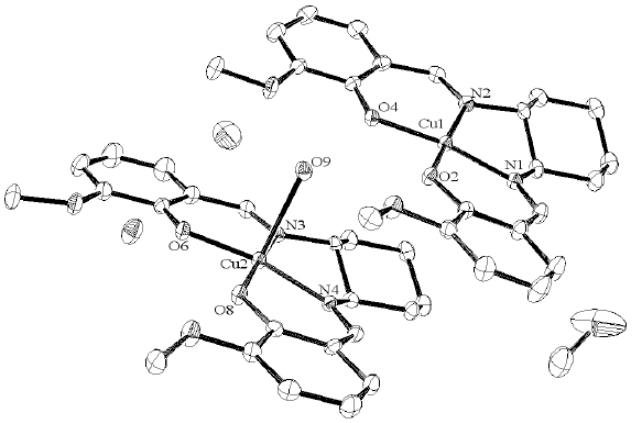

Fig. (2). Molecular structures of **cyCu** showing selected atom labeling scheme. Hydrogen atoms are omitted for clarity.

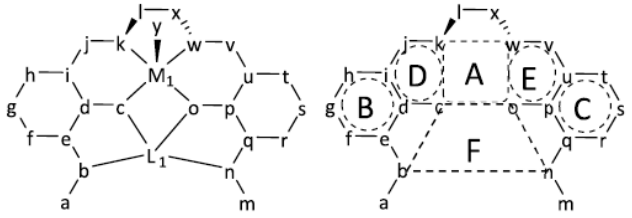

Fig. (3). Definition of mean planes for comparison of common moieties.

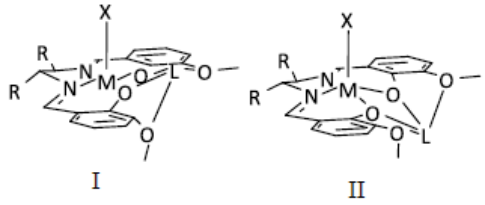

Fig. (4). Distortion of L (I and II distort toward the same side and the opposite side of the axial ligand).

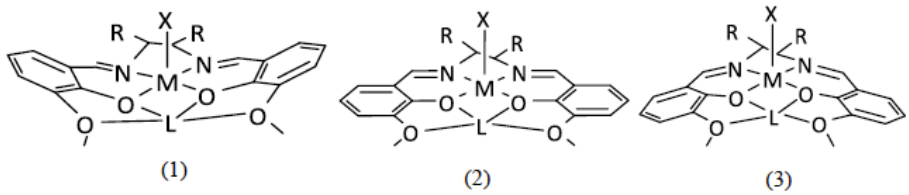

Fig. (5). Distortion of overall molecular structures.

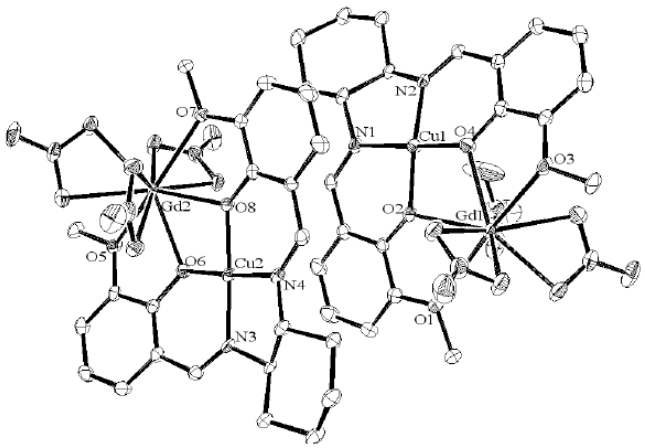

Fig. (6). Molecular structures of **cyGdCu** showing selected atom labeling scheme. Hydrogen atoms are omitted for clarity.

Table 5. Selected bond lengths (Å) and angles(°) for cyGdCu.

Bond lengths			
Cu1-N1	1.916(5)	Cu2-N3	1.919(5)
Cu1-N2	1.912(5)	Cu2-N4	1.923(5)
Cu1-O2	1.898(5)	Cu2-O6	1.912(4)
Cu1-O4	1.911(5)	Cu2-O8	1.906(5)
Gd1-O1	2.554(5)	Gd2-O5	2.575(5)
Gd1-O2	2.332(4)	Gd2-O6	2.404(4)
Gd1-O3	2.635(5)	Gd2-O7	2.545(4)
Gd1-O4	2.335(5)	Gd2-O8	2.334(4)
Bond angles			
N1-Cu1-N2	87.1(2)	N3-Cu2-N4	87.2(2)
N1-Cu1-O2	94.8(2)	N3-Cu2-O6	95.2(2)
N1-Cu1-O4	169.1(2)	N3-Cu2-O8	177.7(2)
N2-Cu1-O2	173.4(2)	N4-Cu2-O6	177.5(2)
N2-Cu1-O4	95.6(2)	N4-Cu2-O8	93.6(2)
O2-Cu1-O4	83.69(19)	O6-Cu2-O8	83.99(18)
O1-Gd1-O2	63.05(16)	O5-Gd2-O6	61.45(14)
O1-Gd1-O3	157.54(15)	O5-Gd2-O7	154.91(15)
O1-Gd1-O4	128.69(15)	O5-Gd2-O8	125.72(15)
O2-Gd1-O3	123.89(16)	O6-Gd2-O7	126.00(14)
O2-Gd1-O4	65.98(17)	O6-Gd2-O8	65.24(15)
O3-Gd1-O4	60.61(15)	O7-Gd2-O8	63.06(15)

The overall molecular structure of planar is an umbrella shape. The dihedral angle between the B-plane and C-plane is 24.82°. The angles between the A-plane and B-plane and between the A-plane and C-plane are 19.18 and 6.45°, respectively. Moreover, the angles between the A-plane and D-plane, between the A-plane and E-planes, and between the D-plane and E-plane are 13.70, 5.94 and, 19.39°, respectively. The displacement of Lu1 from the F-plane is 0.4675(29) Å.

Structure Description of cyCuKNi

Complex **cyCuKNi** crystallizes in triclinic, space group *P*1 with Z = 1. As shown in Figs. (**7** and **S3**), there are four-coordinated and five-coordinated K(I) ions in the same molecule. Moreover, square planar $[Ni(CN)_4]^{2-}$ units are bridged to form a one-dimensional chain as shown in Fig. (**8**). The Cu(II) ion affords a five-coordinated square pyramidal $[CuN_3O_2]$ geometry with Cu1–N1, Cu1-N2, Cu1-O2, and Cu1-O4 distances ranging from 1.885(7) to 1.989(8) Å and the axial Cu1-N5 (cyanide) bond distance being 2.435(8) Å (Table **6**). The displacement of Cu1 from the A-plane (see Fig. **3**) is 0.1640(32) Å. The chiral (*1R,2R*)-(-)-1,2-cyclohexanediamine moiety adopts a λ configuration, with torsion angle N1-C9-C20-N2 =43.1(8)°.

The dihedral angle between the B-plane and C-plane is 6.06°. The angles between the A-plane and B-plane and between the A-plane and C-plane are 9.68, and 3.63°, respectively. Moreover, the angles between the A-plane and D-plane, between the A-plane and E-planes, and between the D-plane and E-plane are 9.49, 4.89, and 6.51°, respectively.

The displacement of K1 from the F-plane is 0.0307(50) Å, and there is K ion almost in the F-plane. Detailed structural description for the other molecules with Cu2 is omitted because of similarity.

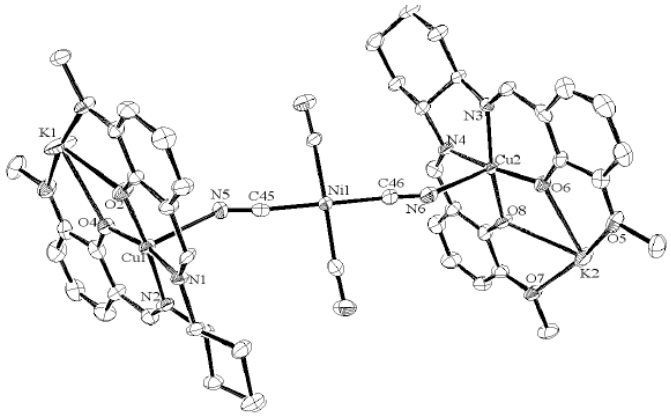

Fig. (7). Molecular structures of **cyCuKNi** showing selected atom labeling scheme. Hydrogen atoms are omitted for clarity.

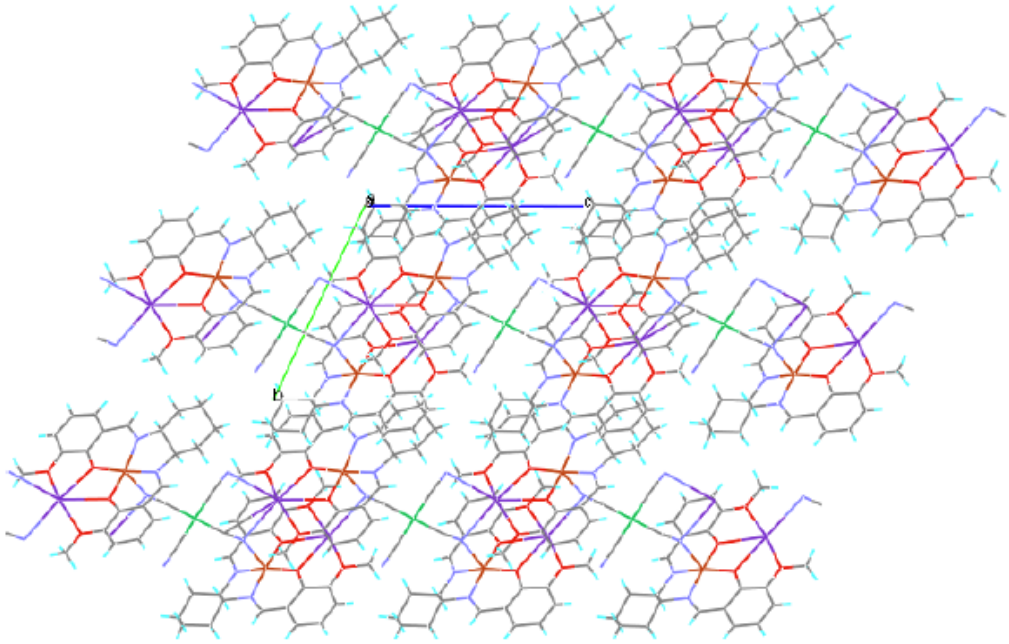

Fig. (8). Crystal packing of **cyCuKNi** viewed down from the *a* axis.

Structure Description of cyLuNi, cyLuCu, and cyLuZn

Complexes ***cyLuNi, cyLuCu, and cyLuZn*** crystallize in triclinic, space group *P*1 with Z = 2, $P2_1$ with Z = 4, and *P*1 with Z = 2, respectively. As shown in Figs. (**9**-**11** and **S4**-**S6**), Lu(III) ion affords a ten-, nine-, and nine-coordinated environment with distorted square pyramidal from the plane made by two nitrate ligands. Ni(II) ion affords a four-coordinated square planar [NiN_2O_2] geometry with Ni1–N1, Ni1-N2, Ni1-O2, and Ni1-O4 distances ranging from 1.814(14) to 1.888(14) Å (Table **7**). Cu(II) ion affords a five-coordinated square pyramidal [CuN_2O_3] geometry with Cu1-N1, Cu1-N2, Cu1-O2, and Cu1-O4 distances ranging from 1.893(5) to 1.920(4) Å and axial O atom from bridging nitrate ligand with Cu1–O9 distance of 2.399(5) Å (Table **8**). Zn(II) ion affords a five-coordinated square pyramidal [ZnN_2O_3] geometry with Zn1–N1, Zn1-N2, Zn1-O2, and Zn1-O4 distances ranging from 2.015(9) to 2.054(9) Å and axial O atom from bridging acetate ligand with Zn1–O9 distance of 1.996(9) Å (Table **9**). The displacement of Ni1, Cu1, and Zn1 atoms from the A-plane (see Fig. **3**) is 0.0071(85) Å, 0.0619(20) Å, and 0.6150(45) Å, respectively. The chiral (*1R,2R*)-(-)-1,2-cyclohexanediamine group adopts a λ configuration, with torsion angle N1-C9-C20-N2 = -43.3(13)°, -42.0(5)°, and -43.4(9)°, respectively.

The dihedral angles between the B-plane and C-plane are 3.08°, 16.91°, and 32.59°, respectively. The angles between the A-plane and B-plane and between the A-plane and C-plane are 8.98, and 6.00°, 10.08, and 10.99°, and 11.36 and 21.32°, respectively. Moreover, the angles between the A-plane and D-plane, between the A-plane and E-planes, and between the D-plane and E-plane are 11.34, 7.41, and 5.59°, 1.44, 9.78, and 11.02°, and 14.07, 23.01, and 37.07°, respectively.

Structure Description of diCu

Complex **diCu** crystallizes in monoclinic, space group $P2_1$ with Z = 4. As shown in Figs. (**12** and **S7**), Cu(II) ion affords a five-coordinated square pyramidal [CuN_2O_3] geometry with Cu1–N1, Cu1-N2, Cu1-O2, Cu1-O4 distances ranging from 1.921(2) to 1.964(3) Å and axial O atom from

Table 6. Selected bond lengths (Å) and angles(°) for cyCuKNi.

Bond lengths			
Cu1-N1	1.934(7)	Cu2-N3	1.907(8)
Cu1-N2	1.989(8)	Cu2-N4	1.964(7)
Cu1-O2	1.885(7)	Cu2-O6	1.915(6)
Cu1-O4	1.927(6)	Cu2-O8	1.941(7)
Cu1-N5	2.435(8)	Cu2-N6	2.403(9)
Ni1-C45	1.822(12)	Ni1-C47	1.861(11)
Ni1-C46	1.912(11)	Ni1-C48	1.861(10)
K1-O1	2.716(7)	K2-O5	2.771(7)
K1-O2	2.696(7)	K2-O6	2.723(7)
K1-O3	2.765(7)	K2-O7	2.727(7)
K1-O4	2.705(7)	K2-O8	2.707(7)
K1-N6$^{\#2}$	2.864(9)	K2-N5$^{\#1}$	2.868(10)
		K2-N8$^{\#1}$	3.170(11)
Bond angles			
N1-Cu1-N2	83.5(3)	N3-Cu2-N4	85.5(3)
N1-Cu1-O2	94.3(3)	N3-Cu2-O6	94.5(3)
N1-Cu1-O4	173.9(3)	N3-Cu2-O8	172.5(3)
N2-Cu1-O2	169.3(3)	N4-Cu2-O6	166.2(3)
N2-Cu1-O4	92.6(3)	N4-Cu2-O8	92.0(3)
O2-Cu1-O4	88.6(3)	O6-Cu2-O8	86.3(3)
C45-Ni1-C46	178.0(6)	C46-Ni1-C47	86.1(4)
C45-Ni1-C47	94.3(4)	C46-Ni1-C48	91.2(4)
C45-Ni1-C48	88.5(5)	C47-Ni1-C48	176.1(6)
O1-K1-O2	57.3(2)	O5-K2-O6	56.5(2)
O1-K1-O3	172.7(2)	O5-K2-O7	164.2(2)
O1-K1-O4	116.4(2)	O5-K2-O8	114.4(2)
O2-K1-O3	115.5(2)	O6-K2-O7	114.4(2)
O2-K1-O4	59.06(19)	O6-K2-O8	58.13(19)
O3-K1-O4	56.6(2)	O7-K2-O8	56.9(2)

Symmetry operation: $^{\#1}$[x, y, -1+z], $^{\#2}$[x, y, 1+z].

coordinate aqua ligand with Cu1–O9 distance of 2.340(3) Å (Table **10**). The displacement of Cu1 atom from the A-plane (see Fig. **3**) is 0.1634(13) Å. The chiral (*1R,2R*)-(+)-1,2-diphenylethylenediamine group adopts a λ configuration, with torsion angle N1-C9-C24-N2 and C10-C9-C24-C25 = -47.6(3)° and 58.0(3)°, respectively.

The dihedral angle between the B-plane and C-plane is 9.00°. The angles between the A-plane and B-plane and between the A-plane and C-plane are 11.36 and 8.44°, respectively. Moreover, the angles between the A-plane and D-plane, between the A-plane and E-planes, and between the D-plane and E-plane are 14.12, 4.90, and 15.02°, respectively.

Two axial water ligands of two molecules face each other inside the two dimeric molecules (see Fig. **4**) and the displacement of O10 from the F-plane is 0.7791(35) Å. The overall molecular structure is slightly distorted umbrella shape to the opposite direction of the axial ligand (see Fig. **5**).

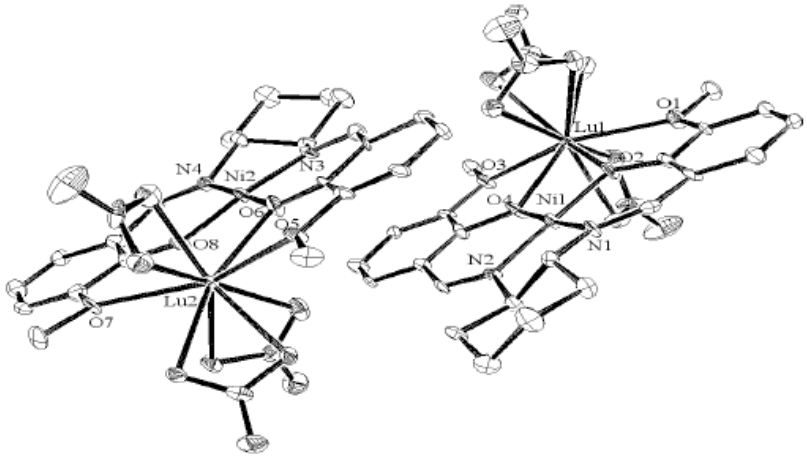

Fig. (9). Molecular structures of **cyLuNi** showing selected atom labeling scheme. Hydrogen atoms are omitted for clarity.

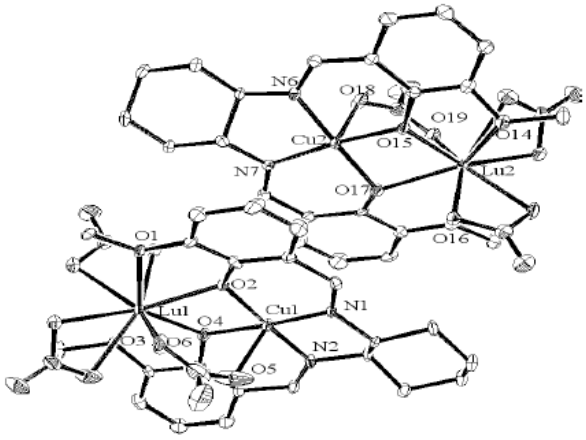

Fig. (10). Molecular structures of **cyLuCu** showing selected atom labeling scheme. Hydrogen atoms are omitted for clarity.

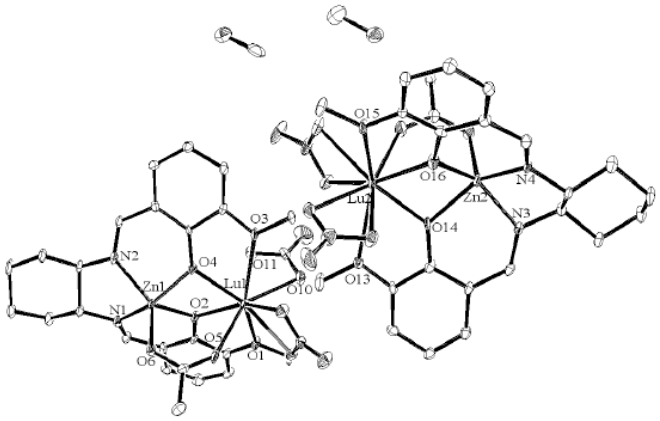

Fig. (11). Molecular structures of **cyLuZn** showing selected atom labeling scheme. Hydrogen atoms are omitted for clarity.

Table 7. Selected bond lengths (Å) and angles(°) for cyLuNi.

Bond lengths			
Ni1-N1	1.848(15)	Ni2-N3	1.836(16)
Ni1-N2	1.857(14)	Ni2-N4	1.852(15)
Ni1-O2	1.888(14)	Ni2-O6	1.861(14)
Ni1-O4	1.814(14)	Ni2-O8	1.806(14)
Lu1-O1	2.477(15)	Lu2-O5	2.523(13)
Lu1-O2	2.287(13)	Lu2-O6	2.338(14)
Lu1-O3	2.451(12)	Lu2-O7	2.471(13)
Lu1-O4	2.302(13)	Lu2-O8	2.270(13)
Bond angles			
N1-Ni1-N2	87.4(6)	N3-Ni2-N4	88.0(7)
N1-Ni1-O2	95.8(6)	N3-Ni2-O6	95.2(7)
N1-Ni1-O4	176.3(6)	N3-Ni2-O8	174.5(7)
N2-Ni1-O2	176.2(6)	N4-Ni2-O6	175.6(7)
N2-Ni1-O4	96.1(6)	N4-Ni2-O8	94.9(6)

(Table 7) contd….

Bond angles			
O2-Ni1-O4	80.9(6)	O6-Ni2-O8	82.2(6)
O1-Lu1-O2	63.6(5)	O5-Lu2-O6	62.6(4)
O1-Lu1-O3	152.2(5)	O5-Lu2-O7	150.2(5)
O1-Lu1-O4	123.0(5)	O5-Lu2-O8	124.3(4)
O2-Lu1-O3	127.4(4)	O6-Lu2-O7	126.5(4)
O2-Lu1-O4	63.1(4)	O6-Lu2-O8	63.1(5)
O3-Lu1-O4	64.8(5)	O7-Lu2-O8	66.4(5)

Table 8. Selected bond lengths (Å) and angles(°) for cyLuCu.

Bond lengths			
Cu1-N1	1.918(4)	Cu2-N3	1.914(4)
Cu1-N2	1.920(4)	Cu2-N4	1.913(4)
Cu1-O2	1.893(5)	Cu2-O6	1.914(4)
Cu1-O4	1.907(4)	Cu2-O8	1.917(5)
Cu1-O9	2.399(5)	Cu2-O18	2.361(4)
Lu1-O1	2.443(4)	Lu2-O5	2.676(4)
Lu1-O2	2.262(3)	Lu2-O6	2.225(4)
Lu1-O3	2.594(4)	Lu2-O7	2.465(4)
Lu1-O4	2.250(4)	Lu2-O8	2.259(3)
Bond angles			
N1-Cu1-N2	87.89(18)	N3-Cu2-N4	86.94(19)
N1-Cu1-O2	94.84(18)	N3-Cu2-O6	95.87(17)
N1-Cu1-O4	175.80(19)	N3-Cu2-O8	178.04(17)
N2-Cu1-O2	173.37(16)	N4-Cu2-O6	169.68(17)
N2-Cu1-O4	95.98(17)	N4-Cu2-O8	94.78(17)
O2-Cu1-O4	81.14(16)	O6-Cu2-O8	82.28(16)
O1-Lu1-O2	65.29(14)	O5-Lu2-O6	61.31(13)
O1-Lu1-O3	154.02(13)	O5-Lu2-O7	155.82(13)
O1-Lu1-O4	131.01(12)	O5-Lu2-O8	124.37(13)
O2-Lu1-O3	125.85(13)	O6-Lu2-O7	133.25(12)
O2-Lu1-O4	66.43(14)	O6-Lu2-O8	68.39(15)
O3-Lu1-O4	62.01(12)	O7-Lu2-O8	64.86(14)

As shown in Figs. (**3**-**5**), the least square mean planes (A-plane , B-plane, C-plane, D-plane, E-plane, and F-plane) are defined using the atom groups (c/k/w/o, d/e/f/g/h/i , p/q/r/s/t/u , c/d/i/j/k ,o/p/u/v/w, and b/c/o/n) for the molecule with M1 atom. Similarly, the least square mean planes (A'-plane , B'-plane, C'-plane, D'-plane, E'-plane, and F'-plane) are defined for the molecule with M atom.

Similar to previous binuclear 3d-4f complexes [10-13, 20-22], Lu(III) ions of most of the complexes described in this paper adopt ten-coordinated environment. However, nine-coordinated Lu(III) ions are also found for **diLuZn** [20], **cyLuCu**, and **cyLuZn**, and both nine- and ten-coordinated Lu(III) ions are found for **diLuCu** [20]. Formation of nine-coordinated Lu(III) environment is attributed to the smallest ionic radii due to lanthanide contraction as well as significantly steric hindrance of nitrate ions to eliminate [10-13, 20-22].

Bridged structures for **cyLuCu**, **cyLuZn**, and **diLuZn** [20] may be ascribed to axial ligands of Cu(II) and Zn(II) complexes. Distortion of Lu(III) coordination environment

Table 9. Selected bond lengths (Å) and angles(°) for cyLuZn.

Bond lengths			
Zn1-N1	2.017(10)	Zn2-N3	2.017(8)
Zn1-N2	2.054(9)	Zn2-N4	2.051(10)
Zn1-O2	2.027(9)	Zn2-O6	2.042(10)
Zn1-O4	2.015(9)	Zn2-O8	1.998(8)
Zn1-O9	1.996(9)	Zn2-O17	1.972(9)
Lu1-O1	2.539(9)	Lu2-O5	2.599(9)
Lu1-O2	2.265(9)	Lu2-O6	2.242(8)
Lu1-O3	2.626(9)	Lu2-O7	2.559(9)
Lu1-O4	2.253(9)	Lu2-O8	2.232(8)
Bond angles			
N1-Zn1-N2	81.8(3)	N3-Zn2-N4	81.6(3)
N1-Zn1-O2	89.0(4)	N3-Zn2-O6	89.7(4)
N1-Zn1-O4	152.0(4)	N3-Zn2-O8	145.3(3)
N2-Zn1-O2	137.1(3)	N4-Zn2-O6	144.3(4)
N2-Zn1-O4	90.8(4)	N4-Zn2-O8	89.9(3)
O2-Zn1-O4	78.1(4)	O6-Zn2-O8	77.8(4)
O1-Lu1-O2	63.1(3)	O5-Lu2-O6	62.2(3)
O1-Lu1-O3	148.5(3)	O5-Lu2-O7	147.6(3)
O1-Lu1-O4	130.8(3)	O5-Lu2-O8	125.2(3)
O2-Lu1-O3	125.4(3)	O6-Lu2-O7	131.8(3)
O2-Lu1-O4	68.6(3)	O6-Lu2-O8	69.1(3)
O3-Lu1-O4	61.9(3)	O7-Lu2-O8	63.4(3)

toward the axial ligand side may be due to stabilization of bond lengths (Fig. **4**). Overall molecular shape also depends on flexibility of 3d ions, namely flexible Cu(II) and Ni(II) for flexible while rigid Zn(II) for bent ones (Fig. **5**).

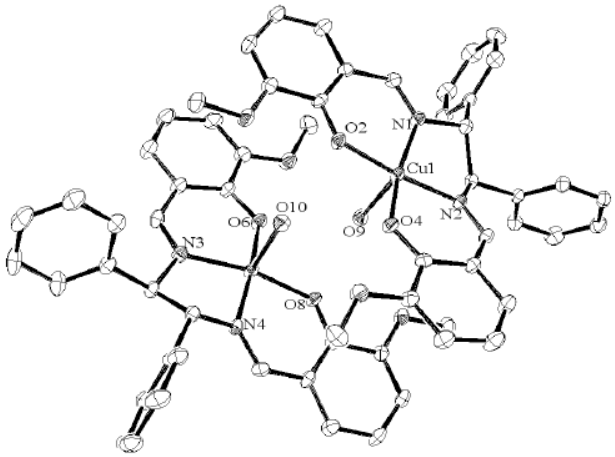

Fig. (12). Molecular structures of **diCu** showing selected atom labeling scheme. Hydrogen atoms are omitted for clarity.

Solid-state CD and Electronic Spectra

Figs. (**13** and **S8**) show CD spectra for **cyCu** and **cyCuKNi** and diffuse reflectance electronic spectra for **cyCu** and **cyCuKNi,** respectively. Figs. (**S9** and **S10**) show CD spectra for **cyLuNi**, **cyLuCu**, and **cyLuZn** and diffuse reflectance electronic spectra for **cyLuNi**, **cyLuCu**, and **cyLuZn**, respectively.

The d-d bands (only for Ni(II) or Cu(II) moieties) and CT bands of CD spectra appeared at about 16000-18000 cm^{-1} and 24500-26800 cm^{-1}, respectively. The corresponding d-d bands of electronic spectra appeared at about 18400-18600 cm^{-1}, the changes of which are attributed to substitution and/or coordination environment of 3d metal ions [20, 21].

Solid-state Fluorescence Spectra

Fig. (**14**) depicts fluorescence spectra of **cyLuZn** at 300 K in the solid states. Under this condition determined based on the electronic spectra, florescence peak for **cyLuZn** appeared at 460 nm due to the ligand. Unfortunately, the other complexes could not be observed in the fluorescence spectra in the solid state under the same conditions.

Table 10. Selected bond lengths (Å) and angles(°) for diCu.

Bond lengths			
Cu1-N1	1.946(2)	Cu2-N3	1.951(3)
Cu1-N2	1.964(3)	Cu2-N4	1.966(3)
Cu1-O2	1.932(2)	Cu2-O6	1.938(2)
Cu1-O4	1.921(2)	Cu2-O8	1.916(2)
Cu1-O9	2.340(3)	Cu2-O10	2.333(3)
Bond angles			
N1-Cu1-N2	83.03(11)	N3-Cu2-N4	83.38(11)
N1-Cu1-O2	92.60(10)	N3-Cu2-O6	92.10(10)
N1-Cu1-O4	173.99(11)	N3-Cu2-O8	172.66(12)
N2-Cu1-O2	164.93(11)	N4-Cu2-O6	166.45(11)
N2-Cu1-O4	92.68(10)	N4-Cu2-O8	92.97(10)
O2-Cu1-O4	90.49(9)	O6-Cu2-O8	90.01(9)

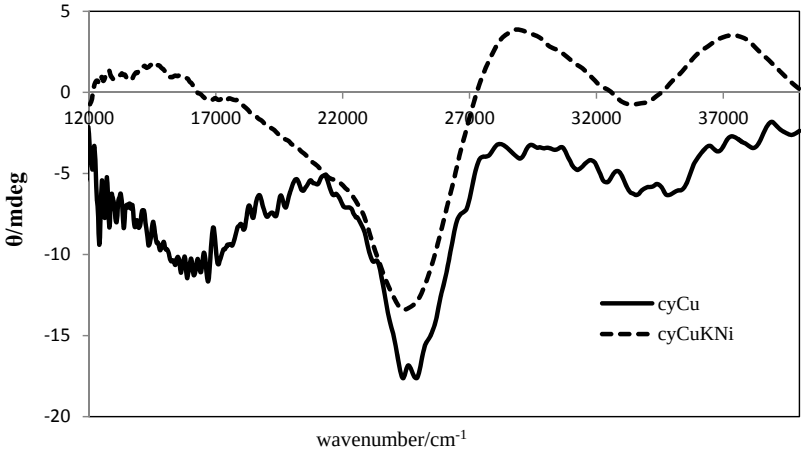

Fig. (13). Solid-state CD spectra for **cyCu**,and **cyCuKNi**.

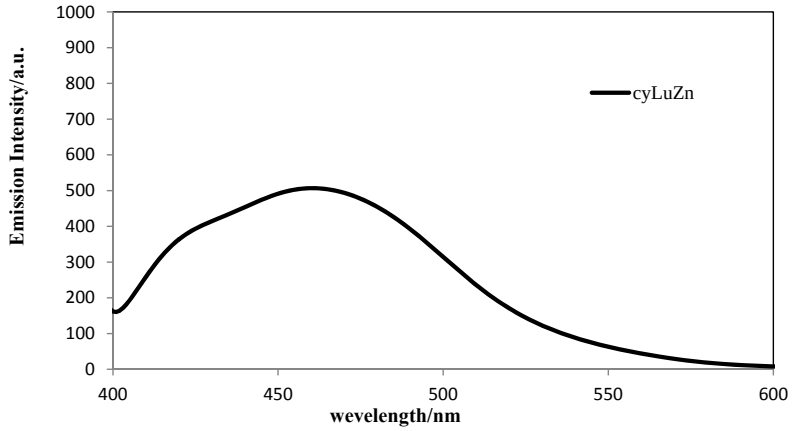

Fig. (14). Solid-state fluorescence spectra (λ_{ex} = 360 nm) for **cyLuZn** at 300 K.

CONCLUSION

Consequently, Fig. (**1**) also summarized structural features for a series of salen-type complexes mentioned. This study systematically reports on Lu(III) complexes (the smallest ion radii among 4f ions) of ten-coordinated for **di-LuNi** [20], **cyLuNi**, nine- and ten-coordinated for **di-LuCu**[20], and nine-coordinated for **cyLuCu**, **cydiZn**, **cy-LuZn**. Therefore, desorption of nitrate ions is facilitated by

significantly steric hindrance. As for 3d ions, axial ligands and degree of distortion from planar basal plane exhibited variety among them. Distortion of overall molecular structures depends on 3d metal ions mainly. So Ni(II) complex is planar, and Zn(II) complex is an umbrella shape toward the opposite direction to the axial ligand. However, as for flexible Cu(II) complex, distortion of overall molecular structures depends on 4f metal ions. Flexibility of coordination environment of Cu(II) ions brings about the diversification of the structures.

CONFLICT OF INTEREST

The authors confirm that this article content has no conflict of interest.

ACKNOWLEDGEMENTS

This work was supported by Research Foundation for Opto-Science and Technology.

SUPPLEMENTARY MATERIAL

CCDC 978339-978345 contain the supplementary crystallographic data. These data can be obtained free of charge via http://www.ccdc.cam.ac.uk/conts/retrieving.html, or from the Cambridge Crystallographic Data Centre, 12 Union Road, Cambridge CB2 1EZ, UK; Fax: (+44) 1223-336-033; or E-mail: deposit@ccdc.cam.ac.uk

REFERENCES

[1] Bryliakov, K.P.; Talsi, E.P. Cr(III)(salen)Cl catalyzed asymmetric epoxidations: insight into the catalytic cycle. *Inorg. Chem.,* **2003**, *42*, 7258-7265.

[2] Jain, S.; Zheng, X.; Jones, CW.; Weck, M.; Davis, R.J. Importance of counterion reactivity on the deactivation of co-salen catalysts in the hydrolytic kinetic resolution of epichlorohydrin. *Inorg. Chem.,* **2007**, *46*, 8887-8896.

[3] Adao, P.; Pessoa, J.C.; Henriques, R.T.; Kuznetsov, M.L.; Avecilla, F.; Maurya, M.R.; Kumar, U.; Correia, I. Synthesis, characterization, and application of vanadium-salan complexes in oxygen transfer reactions. *Inorg. Chem.,* **2009**, *48*, 3542-3561.

[4] Oxford, G.A.E.; Snurr, R.Q.; Broadbelt, L.J. Hybrid quantum mechanics/molecular mechanics investigation of (salen)Mn for use in metal-organic frameworks. *Ind. Eng. Chem. Res.,* **2010**, *49*, 10965-10973.

[5] Zhao, Z.P.; Li, M.S.; Zhang, J.Y.; Li, H.N.; Zhu, P.P.; Liu, W.F. New chiral catalytic membranes created by coupling uvphotografting with covalent immobilization of salen−Co(III) for hydrolytic kinetic resolution of racemic epichlorohydrin. *Ind. Eng. Chem. Res.,* **2012**, *51*, 9531-9539.

[6] Kurahashi, T.; Hada, M.; Fujii, H. Critical role of external axial ligands in chirality amplification of trans-cyclohexane-1,2-diamine in salen complexes. *J. Am. Chem. Soc.,* **2009**; *131*, 12394-12405.

[7] Nielsen, L.P.C.; Zuend, S.J.; Ford, D.D.; Jacobsen, EN. Mechanistic basis for high reactivity of (salen)Co−OTs in the hydrolytic kinetic resolution of terminal epoxides. *Org. Chem.,* **2012**; *77*, 2486-2495.

[8] Xu, L.; Zhang, Q.; Hou, G.; Chen, P.; Li, G.; Pajerowski, D.M.; Dennis, C.L. Syntheses, structures, and magnetic properties of salen type Cu–Gd dimer and hexamer complexes with strong ferromagnetic interactions. *Polyhedron.*, **2013**; *52*, 91-95.

[9] Sui, Y.; Liu, D.S.; Hu, R.H.; Huang, J.G. One-dimensional zigzag chain of Cu–Gd coordination polymers derived from chiral hexadentate Schiff base ligands: Synthesis, structure and magnetic properties. *Inorg. Chem. Acta.,* **2013**, *395*, 225-229.

[10] Koner, R.; Lee, G.H.; Wang, Y.; Wei, H.H.; Mohanta, S. Two new diphenoxo-bridged discrete dinuclear Cu(II)Gd(III) compounds with cyclic diimino moieties: syntheses, structures, and magnetic properties. *Eur. J. Inorg. Chem.,* **2005**, *8,* 1500-1505.

[11] Costes, J.P.; Dahan, F.; Dupuis, A. Influence of anionic ligands (x) on the nature and magnetic properties of dinuclear $LCuGdX_3{\cdot}nH2O$ complexes (LH_2 standing for tetradentate schiff base ligands deriving from 2-hydroxy-3-methoxybenzaldehyde and X being Cl, N_3C_2, and CF_3COO). *Inorg. Chem.,* **2000**, *39*, 165-168.

[12] Margeat, O.; Acroix, P.G.; Costes, J.P.; Donnadieu, B.; Lepetit, C. Synthesis, structures, and physical properties of copper(II)-gadolinium(III) complexes combining ferromagnetic coupling and quadratic nonlinear optical properties. *Inorg. Chem.,* **2004**, *43*, 4743-4750.

[13] Jana, A.; Majumder, S.; Carrella, L.; Nayak, M.; Weyhermueller, T.; Dutta, S.; Schollmeyer, D.; Rentschler, E.; Koner, R.; Mohanta, S. Syntheses, structures, and magnetic properties of diphenoxo-bridged Cu(II)Ln(III) and NiII(low-spin)Ln(III) compounds derived from a compartmental ligand (Ln = Ce-Yb). *Inorg. Chem.,* **2010**, *49*, 9012-9025.

[14] Wong, W.K.; Yang, X.; Jones, R.A.; Rivers, J.H.; Lynch, V.; Lo, W.K.; Xiao, D.; Oye, M.M.; Holmes, A.L. Multinuclear luminescent schiff-base Zn-Nd sandwich complexes. *Inorg. Chem., **2006**, 45*, 4340-4345.

[15] Pasatoiu, T.D.; Madalan, A.M.; Kumke, M.U.; Tiseanu, C.; Andruh, M. Temperature switch of LMCT role: from quenching to sensitization of europium emission in a Zn(II)-Eu(III) binuclear complex. *Inorg. Chem.,* **2010**, *49*, 2310-2315.

[16] Pasatoiu, T.D.; Sutter, J.P.; Madalan, A.M.; Zohra, F.; Fellah, C.; Duhayon, C.; Andruh, M. Preparation, crystal structures, and magnetic features for a series of dinuclear [Ni(II)Ln(III)] schiff-base complexes: evidence for slow relaxation of the magnetization for the Dy(III) derivative. *Inorg. Chem.,* **2011**, *50*, 5890-5898.

[17] Andruh, M.; Costes, J.P.; Diaz, C.; Gao, S. 3d-4f combined chemistry: synthetic strategies and magnetic properties. *Inorg. Chem.,* **2009**, *48*, 3342-3359.

[18] Pasatoiu, T.D.; Tiseanu, C.; Madalan, A.M.; Jurca, B.; Duhayon, C.; Sutter, J.P.; Andruh, M. Study of the luminescent and magnetic properties of a series of heterodinuclear [Zn(II)Ln(III)] complexes. *Inorg. Chem.,* **2011**, *50*, 5879–5889.

[19] Lo, W.K.; Wong, W.K.; Wong, W.Y.; Guo, J.; Yeung, K.T.; Cheng, Y.K.; Yang, X.; Jones, R.A. Heterobimetallic Zn(II)-Ln(III) phenylene-bridged schiff base complexes, computational studies, and evidence for singlet energy transfer as the main pathway in the sensitization of near-infrared Nd^{3+} luminescence. *Inorg. Chem.,* **2006**, *45*, 9315-9325.

[20] Hayashi, T.; Shibata, H.; Orita, S.; Akitsu, T. Variety of structures of binuclear chiral schiff base Ce(III)/Pr(III)/Lu(III)-Ni(II)/Cu(II)/Zn(II) complexes. *Eur. Chem. Bull*., **2013**, *2*, 49-57.

[21] Akitsu, T.; Hirarsuka, T.; Shibata, H. Chiroptical properties of 3d-4f chiral Schiff base magnetic complexes. Magnets:Types, Uses and Safety, Nova Science Publishers, **2012**: 69-84.

[22] Okamoto, Y.; Nidaira, K.; Akitsu, T. Environmental dependence of artifact CD peaks of chiral schiff base 3d-4f complexes in soft mater PMMA matrix. *Int. J. Mol. Sci.,* **2011**, *12*, 6966-6979.

[23] Akitsu, T. New attempt of empirical approach for magnetic interactions: several examples of 3d-4f $[Ln(DMA)_2(H_2O)_4M(CN)_6{\cdot}5H_2O]_n$ bimetallic assemblies (DMA = *N,N*-dimethylacetamide). *Asian. Chem. Lett.,* **2010**, *14*, 53-62.

[24] Sheldrick, G.M. A short history of SHELX. *Acta. Crystallogr. A*., **2008**, *64*, 112-22.

Received: June 16, 2014 Revised: August 04, 2014 Accepted: August 11, 2014